



High-pressure homogenization to improve the stability of liquid diabetes formula food for special medical purposes: Structural characteristics of casein–polysaccharide complexes

Xueting Zheng^{a,b,1}, Zengwang Guo^{b,1}, Jiayu Zhang^b, Tianfu Cheng^b, Hong Yang^c, Wentao Zhang^{a,d,*}, Linyi Zhou^{a,**}

^a School of Food and Health, Beijing Technology and Business University, Beijing 100048, PR China

^b College of Food Science, Northeast Agricultural University, Harbin, Heilongjiang 150030, China

^c Libang Clinical Nutrition Co., Ltd., Xi'an, Shanxi 710065, China

^d Key Laboratory of Green and Low-carbon Processing Technology for plant-based Food of China National Light Industry Council, Beijing 100048, PR China

ARTICLE INFO

Keywords:

Medical foods
High-pressure homogenization
Casein
Complexes
Interface
Stability

ABSTRACT

The stability of diabetes formula food for special medical purposes (D-FSMP) was improved by high-pressure homogenization (HPH) at different homogenization pressures (up to 70 MPa) and number of passes (up to 6 times). The process at 60 MPa/4 times was the best. Casein had the highest surface hydrophobicity in this condition. The casein–polysaccharide complexes were endowed with the smallest size (transmission electron microscopy images). The complex particles exhibited nearly neutral wettability (the three-phase contact angle was 90.89°), lower interfacial tension, and the highest emulsifying activity index (EAI) and emulsifying stability index (ESI). The prepared D-FSMP system exhibited the narrowest particle size distribution range, the strongest interfacial deformation resistance and the best storage stability. Therefore, an appropriate intensity of HPH could enhance the stability of D-FSMP by improving the interfacial and emulsifying properties of casein–polysaccharide complexes. This study provides practical guidance on the productions of stable D-FSMP.

1. Introduction

Formula food for special medical purposes (FSMP) is a special food category that has evolved with the progress of the times, the development of medicine and the needs of society. FSMP is also called medical foods. For patients diagnosed with malnutrition by doctors or clinical nutritionists, tube feeding or oral nutritional supplement are two ways for FSMP to deliver nutrition (Ruperto et al., 2022). These patients are mainly people with certain illnesses or special health conditions, such as diabetes patients (Huang, Lu, Shi, & Zhang, 2023). Over the past few decades, diabetes has emerged as a significant public health concern in China. The incidence and prevalence of the diabetes are rising steadily, impacting the physical and mental well-being of the population (Chinese Diabetes Society, & National Office for Primary Diabetes Care, 2022). In the hospitalization of diabetes patients, medical nutrition therapy is

deemed crucial. The diabetes formula food for special medical purposes (D-FSMP) is a type of specialized medical nutrition for diabetes. It is also identified as the most effective and direct approach to maintain and improve the nutritional status, quality of life, and physiological health of diabetes patients (Stippler et al., 2015). Compared with ordinary enteral nutrition preparations, D-FSMP has more advantages in terms of controlling blood sugar and reducing insulin usage in critically ill patients (Pohl et al., 2005). For instance, D-FSMP is more focused on decreasing the metabolic burden, enhancing nutritional orientation, and thus reducing the harm of dietary taboos (Casale et al., 2021). At present, D-FSMP dosage forms include solid, semi-solid, liquid, and powder. Among them, liquid dosage forms are more widely used because they are easy to digest and highly safe and could be directly tube-fed or taken orally (Wu, Zhang, & Zhang, 2019).

The liquid diabetes formula food for special medical purposes is

* Corresponding author at: Key Laboratory of Green and Low-carbon Processing Technology for plant-based Food of China National Light Industry Council, Beijing 100048, PR China.

** Corresponding author.

E-mail addresses: zhangwentao_14@126.com (W. Zhang), dorisneau@126.com (L. Zhou).

¹ These authors contributed equally to this work.

characterized by a complex oil-in-water (O/W) emulsion system. In this system, protein is an essential nutrient for patients with diabetes, and polysaccharides are mainly used as thickeners to improve product stability. The stability of O/W emulsion has been elucidated by many researchers, revealing that the emulsification of a single protein is constrained and the emulsion is prone to stratification (Dai et al., 2024). In emulsion food formulations, proteins and polysaccharides work together to improve product stability, flavor, and texture because of their interactions with each other (Burgos-Díaz, Wandersleben, Marqués, & Rubilar, 2016). Casein has been the most often used protein raw material in the D-FSMP system. It is a proline-rich protein with unique hydrophobic and hydrophilic domains. As per previous studies, the inclusion of polysaccharides could enhance the amphiphilic properties of casein, thus increasing the adsorption capacity of casein at the oil–water interface (Machado, Benyahia, & Nicolai, 2021). Simultaneously, the polysaccharides could boost emulsion stability by increasing viscosity, electrostatic interactions, and steric repulsion among droplets (Tao et al., 2024). Carrageenans are sulfated linear polysaccharides consisting of d-galactose and 3,6-anhydro-D-galactose. While the inclusion of carrageenans improved the amphiphilicity and solubility of casein, issues such as poor flexibility and low water-holding capacity persisted. Combining carrageenans with different polysaccharides has helped overcome these problems. It had been proved that xanthan gum and carrageenans had a synergistic effect in emulsion systems (Aljewicz, Keklik, Recio, & Martínez-Sanz, 2024). Xanthan gum, produced and extracellularly released by the microorganism *Xanthomonas campestris*, can lower the concentration at which carrageenans form a gel and enhance water retention, softness, and mouthfeel. Thus, carrageenans and xanthan gum were indispensable excipients in the industrial production of D-FSMP. Additionally, recent studies showed that carrageenans can inhibit the formation of advanced glycation end products in the heat-processed food, thereby decreasing the health risks related to diabetic complications (Wang et al., 2023). Xanthan gum decreases postprandial blood glucose (Nagasawa et al., 2022). However, during storage, the droplets collide due to gravity, Brownian motion, and external mechanical forces. The occurrence of physical instability issues in D-FSMP was observed, including flocculation, fat floating, phase separation, and aggregation (Cámara-Martos & Iturbide-Casas, 2019). Therefore, the feasibility of using D-FSMP is restricted.

The current research focuses on using physical technological approaches to make D-FSMP more stable and resistant to storage. Since they come with higher food safety and industrial application values, for example, ultrasonication, pulsed electric fields, high-pressure microfluidization, and high-pressure homogenization (HPH) (Yu, Wu, & Fan, 2024). Especially, HPH has become a common method in the food industry to produce stable emulsions. Because its technology is the most mature and is well applicable compared with others. The HPH facilitated the passage of the emulsion through narrow, specifically shaped channels at high velocities, thus resulting in a significant reduction in the particle size of emulsion. This could facilitate the production of a more stable emulsion system. Moreover, HPH could improve the protein structure and functional properties, which could be used to produce a more stable emulsion system (Plazzotta, Moreton, Calligaris, & Manzocco, 2021). Therefore, based on the current hardware status of the FSMP industry in China, HPH is particularly suitable for stabilizing D-FSMP. Yu et al. (2024) evaluated the potential application of shear technology in total nutrition lotion system. However, the application of HPH for the D-FSMP system is rarely reported. The impact of HPH on the stability of D-FSMP system and the associated mechanisms are still worth exploring.

In the development and pilot production of D-FSMP products, it has been noted that HPH treatment can cause significant differences in terms of product storage stability. In this study, the effects of different HPH intensities on the structure characteristics of casein–polysaccharide complexes were evaluated. This included 2 times at 60 MPa, 4 times at 60 MPa, 6 times at 60 MPa, 4 times at 30 MPa, 4 times at 50 MPa, and 4

times at 70 MPa. The effects of different HPH intensities on the structure of casein–polysaccharide complexes were evaluated by Fourier transform infrared spectroscopy (FTIR), endogenous fluorescence spectroscopy, surface hydrophobicity (H_0), disulfide bonds and transmission electron microscopy (TEM). The contact angle (θ), interfacial tension, emulsifying activity index (EAI), and emulsifying stability index (ESI) were analyzed to characterize the interfacial and emulsifying properties of complexes. Finally, changes with regard to the particle size, zeta-potential, viscosity, rheological properties, and microstructure of the D-FSMP system were examined to determine the contribution of different HPH intensities to the stabilization mechanism of D-FSMP.

2. Materials and methods

2.1. Materials

Casein was purchased from Lanzhou Longruan Casein Co., Ltd. (Lanzhou, China). Food-grade maltodextrin, xanthan gum, and carrageenans were purchased from Danisco (Wilmington, DE, USA). Fresh linseed oil, rapeseed oil, and corn oil were purchased from a crude oil factory. Fructose was purchased from Syarikat System Malaysia. Resistant dextrin was purchased from Esaki Glico Co., Ltd. (Shanghai, China). All chemicals used were of analytical reagent grade.

2.2. Preparation of casein–polysaccharide complexes

Casein (5.38 wt%), xanthan gum (0.003 wt%), and carrageenans (0.003 wt%) samples were added to deionized water (60 °C) and stirred at 600 rpm for 2 h. Thereafter, the samples were treated under different homogenization pressures (30 MPa, 50 MPa, 60 MPa, and 70 MPa) and number of passes (2 times, 4 times, 6 times) using high-pressure homogenizer (GYB180-18D, Shanghai Donghua High Pressure Homogenizer Factory, Shanghai, China). The samples treated with different HPH intensities were labeled as 60 MPa/2, 60 MPa/4, 60 MPa/6, 30 MPa/4, 50 MPa/4 and 70 MPa/4. The sample without HPH treatment was the control.

2.3. Preparation of D-FSMP

During the preparation of D-FSMP, all substances were precisely measured based on the prescribed amount in the formula (Supplementary Table S1). At 60 °C, maltodextrin, resistant dextrin, fructose, and other materials were dissolved in ultra-purified water. Subsequently, the solution was mixed with casein–polysaccharide (Section 2.2) and supplemented with vegetable oil and multivitamins. A disperser was employed for initial emulsification (2800 r/min, 3 min), followed by homogenization using a high-pressure homogenizer (60 MPa, 4 times). In order to prepare the samples for subsequent use, the samples were canned and subjected to a temperature of 121 °C for 15 s for rapid cooling, and stored at room temperature.

2.4. Structural properties of casein–polysaccharide complexes

2.4.1. Transmission electron microscopy (TEM) measurement

The 0.5 mg/mL solution of casein–polysaccharide complexes was applied to the nickel mesh membrane, followed by rinsing with 10 L of distilled water and staining with 10 L of 2% uranyl acetate for 3 min. In each step, filter paper was used to absorb the excess liquid. The sample film was dried for 15 min at room temperature and then observed using a JEM-1011 transmission electron microscope (JEOL Co., Ltd., Japan) at a 10,000× magnification.

2.4.2. Intrinsic fluorescence spectroscopy measurement

According to the method of Bakwo Bassogog, Nyobe, Ngui, Minka, and Mune Mune (2022), a fluorescence spectrophotometer (RF-6000, Hitachi Ltd., Tokyo, Japan) was used to obtain the fluorescence emission

spectrum of casein–polysaccharide complexes solution at room temperature (25 °C). The excitation wavelength was set at 280 nm, whereas the emission wavelength was set at 290–450 nm. The voltage and slit width were set to 500 mV and 5 nm, respectively.

2.4.3. Surface hydrophobicity (H_0) measurement

The method of Cheng et al. (2024) was used. To prepare the casein–polysaccharide complexes solution, a protein concentration of 5 mg/mL was taken. Next, a solution of casein–polysaccharide was prepared by diluting it with phosphate buffer to concentrations between 0.2 mg/mL and 1 mg/mL. A 20 μ L ANS solution with a concentration of 8 mM was made in the same buffer and then added to 4 mL samples of casein–polysaccharide complexes with varying concentrations. Subsequently, the blend was completely mixed together and kept in the dark for 15 min at room temperature (25 °C). The fluorescence intensity from an external source was determined using a fluorescence spectrophotometer (RF-6000, Hitachi Ltd., Tokyo, Japan), with an excitation wavelength of 390 nm, and the emission spectrum was recorded at 495 nm. The H_0 value was calculated based on the slope of the regression curve, which correlated fluorescence levels with protein amounts.

2.4.4. Fourier transform infrared spectroscopy (FTIR) measurement

The casein–polysaccharide complexes solution was freeze-dried, and the resulting powder was analyzed with STA-6000 FTIR from PerkinElmer (United States). Prior to detection, 2 mg of the sample was combined with KBr at a 1:100 ratio and then compressed it into a solid and translucent flake. Following this, 32 quick scans were conducted between 4000 and 400 cm^{-1} to examine alterations in the sample's structure (Tian et al., 2022).

2.4.5. Disulfide-bond measurement

To determine free-sulfhydryl groups, 3 mL of 1 mg/mL casein–polysaccharide complexes solution was pipetted into a 10 mL test tube. Subsequently, 5 mL of Tris-glycine buffer solution (the solution contained 0.086 mol/L Tris, 0.09 mol/L glycine, and 4 mmol/L EDTA and was mixed well and adjusted to pH 8.0) was added, followed by 0.1 mL of Ellman's reagent. The reaction was thoroughly mixed at 25 °C for 15 min. The absorbance at 412 nm was measured using a UV–vis spectrophotometer (Agilent Cary 60, Agilent, USA).

To determine total-sulfhydryl groups, 5 mL of Tris-glycine buffer solution was replaced with 5 mL of Tris-glycine-8 M Urea-0.5% SDS buffer, and 0.1 mL β -mercaptoethanol was added to the above mixture. The free-sulfhydryl groups (FS), the total-sulfhydryl (TS) and disulfide bonds (DB) were calculated according to the following equation:

$$FS(\mu\text{mol/g}) = (73.53 \times D \times A_{412})/C \quad (1)$$

$$TS(\mu\text{mol/g}) = (73.53 \times D \times A_{412})/C \quad (2)$$

$$DB(\mu\text{mol/g}) = (TS - FS)/2 \quad (3)$$

where 73.53 is the extinction coefficient, D is the dilution coefficient of casein–polysaccharide complexes solution, A_{412} is the absorbance, and C is the concentration of casein (mg/mL).

2.5. Interfacial properties of casein–polysaccharide complexes

2.5.1. Contact angle (θ) measurement

The contact angle of casein–polysaccharide complexes solution was measured using the sessile drop method with a video-based optical goniometer (DSA 25, Krüss GmbH, Hamburg, Germany). The casein–polysaccharide freeze-dried powder should be pressed into pellets measuring 1 cm in diameter and 2 mm in thickness with a tablet press before measurement. The sheet sample was placed in a measuring vessel filled with soybean oil and suspended in deionized water with a volume of about 5 μ L.

2.5.2. Interfacial tension measurement

The interfacial tension of the samples was tested using the sessile drop method with a video-based optical goniometer (DSA 25, Krüss GmbH, Hamburg, Germany). Interfacial tension analysis was performed as previously described by Zhang, Wu, Yang, He, and Wang (2012) with minor modifications. The casein–polysaccharide complexes solution was placed in an instrument syringe, followed by placing a droplet of the solution on the tip of the syringe (5 μ L). Interfacial tension was calculated using the SCA20 software system.

2.5.3. Emulsifying activity index (EAI) and emulsifying stability index (ESI) measurement

Soybean oil (4 mL) and casein–polysaccharide complexes solution (12 mL; 0.5 mg/mL) were mixed, and a disperser was used for high-speed shearing at a rotation speed of 10,000 r/min for 2 min. An aliquot (50 μ L) of the resulting emulsion was then mixed with 5 mL of SDS solution (0.10%). A_0 represents the absorbance at 500 nm, whereas A_t represents the absorbance after 10 min of standing. The calculation formulas of EAI and ESI are as follows:

$$EAI(\text{m}^2/\text{g}) = (2 \times 2.303 \times N \times A_0)/(C \times \varphi \times L \times 10000) \quad (4)$$

$$ESI(\text{min}) = (10 \times A_0)/(A_0 - A_t) \quad (5)$$

where N is the dilution factor; C is the sample concentration, mg/mL; φ is the ratio of the oil phase; and A_0 and A_t represent the absorbance of the samples at 0 min and 10 min, respectively.

2.6. Effect of casein–polysaccharide complexes on D-FSMP system stability

2.6.1. Particle-size measurement

The particle size of D-FSMP samples was measured using Mastersizer 3000 (Malvern Instruments, UK). Refractive indices of 1.414 and 1.330 were used for the oil phase and aqueous phase, respectively. The adsorption index was set as 0.001 and 0.

2.6.2. Zeta-potential measurement

The ζ -potential values of the droplets in D-FSMP were measured using a zeta-potential analyzer (Zeta Plus, Malvern, U.K.) at 25 °C. Specifically, deionized water was used to dilute the D-FSMP products 100 times prior to measurement.

2.6.3. Rheological property measurement

The rheological behaviors of the D-FSMP samples were investigated using an AR 2000ex rheometer (TA Instruments, Crawley, UK). First, 10 mL of the samples was loaded on the steel parallel plate of the rheometer and equilibrated at 25 °C for 5 min. Next, changes in the emulsion viscosity were measured at a shear rate range of 0.1–100 s^{-1} . In addition, the storage (G') and loss (G'') moduli of the emulsion were measured in the linear viscoelastic region at 1 Pa with a frequency range of 0.1–100 Hz.

2.6.4. Cryo-SEM measurement

Cryo-SEM measurement was conducted using Hitachi SU8010 (Hitachi, Tokyo, Japan). The D-FSMP samples were quickly frozen using liquid nitrogen and were sliced. Afterward, the samples were sublimated and treated by sputter coating with platinum and placed in a cold module chamber for examination (Lu, Zhang, Yuan, Gao, & Mao, 2021).

2.7. Appearance changes of D-FSMP after storage

All D-FSMP samples prepared as described in Section 2.3 were stored at room temperature for 1 month. Photographs of the samples were taken through a phone camera (iPhone 14, Apple, Inc., CA, USA) to examine the appearance of D-FSMP.

2.8. Statistical analysis

Three independent measurements were conducted on the same sample. The results were presented as mean with standard deviation (SD). One-way analysis of variance with Duncan's test with a significance level of $P < 0.05$ was performed on the data using the IBM SPSS 23.0 statistical software program (SPSS, Inc., Chicago, IL, USA).

3. Results and discussion

3.1. Structural properties of casein–polysaccharide complexes

3.1.1. Transmission electron microscopy (TEM)

One of the prerequisites for food-grade particle-stabilized emulsions is a good dispersion state. TEM was used to visually observe the micromorphology and particle size of the casein–polysaccharide complexes (Fig. 1). The control evinced a relatively large cluster of aggregates and less ordered structure. In comparison to the control group, it was obvious that the size of casein–polysaccharide complexes particles decreased initially and then increased with an increasing HPH intensity. In the image of the sample treated at 60 MPa/4 times, the separation spheres were smaller and uniform, indicating a better dispersion system. It was demonstrated that HPH treatment improved the solubility of casein–polysaccharide complexes and promoted the development and hydrolysis of complexes, thus contributing to the reduction of particle sizes and improved dispersion stability. The research by Jiang et al. (2024) reported that physical processing can lead to a change in the lactoferrin structure, resulting in a tight binding between lactoferrin and polysaccharides and the formation of more stable and compact complexes in the dispersion. Combined with the previous results (SEC-HPLC, FTIR, fluorescence emission spectra, H_0 , and disulfide bonds), HPH treatment promoted the fragmentation of the protein structure (Cheng, Tian, et al., 2024). This achieved a casein–polysaccharide complex system with a small size, dense structure, and uniform dispersion. Furthermore, the TEM images revealed the formation of some larger spherical aggregates in the samples treated at 60 MPa/6 times and 70 MPa/4 times.

3.1.2. Intrinsic fluorescence spectroscopy analysis

Fluorescence emission spectroscopy is an effective method to analyze the polarity change of the microenvironment around the aromatic ring fluorophore (mainly tryptophan) in proteins. This could be used to examine the conformational changes of casein and identify the presence of the casein–polysaccharide complexes (Yin, Gao, Wang, Chen, & Kong,

2022). As shown in Fig. 2A, the fluorescence intensity (I_{\max}) of casein was significantly enhanced ($P < 0.05$) with HPH treatment, in contrast to the control. This indicates that HPH changed the tertiary structures of casein. With an increase in HPH intensity, the I_{\max} of casein first decreased and then increased, whereas the λ_{\max} decreased (blue shift) first and then increased (red shift). The increase in I_{\max} could be explained by the partial and complete unfolding of the protein structure (Karabulut, Kapoor, Yemis, & Feng, 2024). Consequently, it led to a rise in the number of chromophores exposed to the environment. The decrease of I_{\max} suggested that the polysaccharides in the D-FSMP system form complexes with casein through covalent or non-covalent interactions. This led to a change in the environmental polarity of tryptophan, the tryptophan to be masked. The blue shift of λ_{\max} suggested that the aromatic residues moved to an environment with stronger hydrophobicity inside casein. For high-intensity HPH, the combination of high shear forces with heat likely disrupted hydrogen and hydrophobic interactions ultimately leading to the destabilization of the tertiary structure of casein. The exposure of additional tryptophan (Trp) residues in a relatively hydrophobic setting. Therefore, based on TEM images, it is speculated that the condition of 60 MPa/4 times is more conducive to the rapid formation of a “shell” layer with polysaccharide molecules around casein molecules, thereby inhibiting the aggregation of casein molecules.

3.1.3. Surface hydrophobicity (H_0) analysis

H_0 reflected the density of hydrophobic groups exposed on the surfaces of protein molecules. It could further monitor the changes in the tertiary and quaternary structures of protein. As shown in Fig. 2B, with increasing HPH intensity, H_0 of the sample tended to first increase and then decrease. The sample treated at 60 MPa/4 times showed the highest H_0 value. Evidently, the vigorous mechanical forces of HPH (pressure, shear, turbulence, and cavitation) led to the exposure of additional hydrophobic areas that were initially concealed within casein. The increase in H_0 benefited the rapid and effective uptake of casein at the interface by reducing interfacial tension owing to the enhanced attraction between hydrophobic areas and the nonpolar oil phase (Wang, Tang, Cao, Ming, & Wu, 2024). This might help improve the emulsifying properties of casein. In contrast, the decrease in H_0 was attributed to casein aggregation, which reduced the binding likelihood of ANS probe to hydrophobic amino acid residues. Interestingly, the shift in the H_0 of casein–polysaccharide complexes showed an inverse relation to I_{\max} and mainly corresponded to λ_{\max} . There were many other residues in the hydrophobic amino acid residues of casein besides the aromatic ring residues. This could be a plausible explanation for the difference.

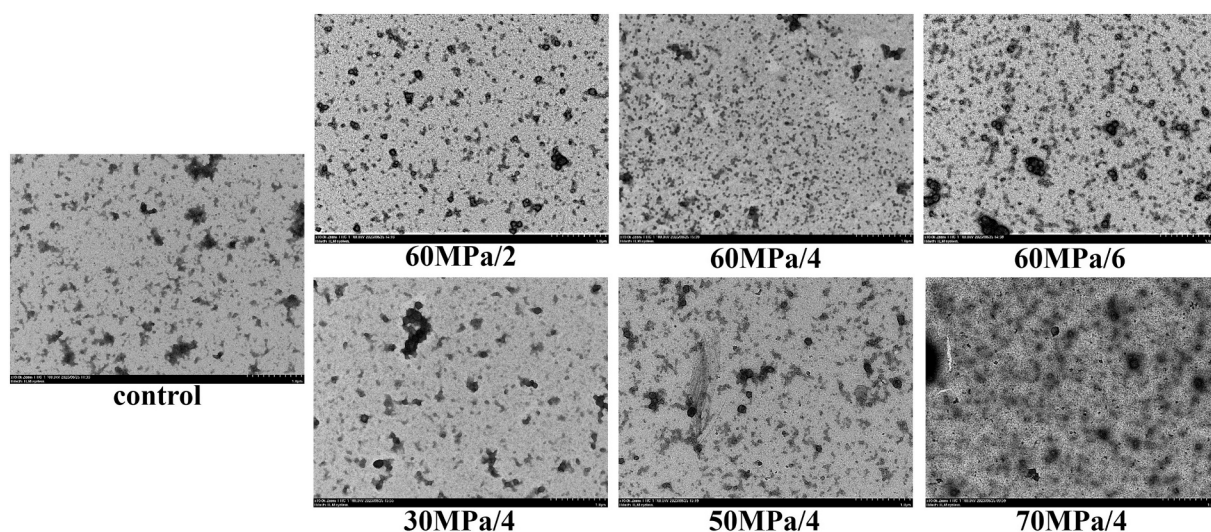


Fig. 1. TEM images of casein–polysaccharide complexes under different HPH intensities.

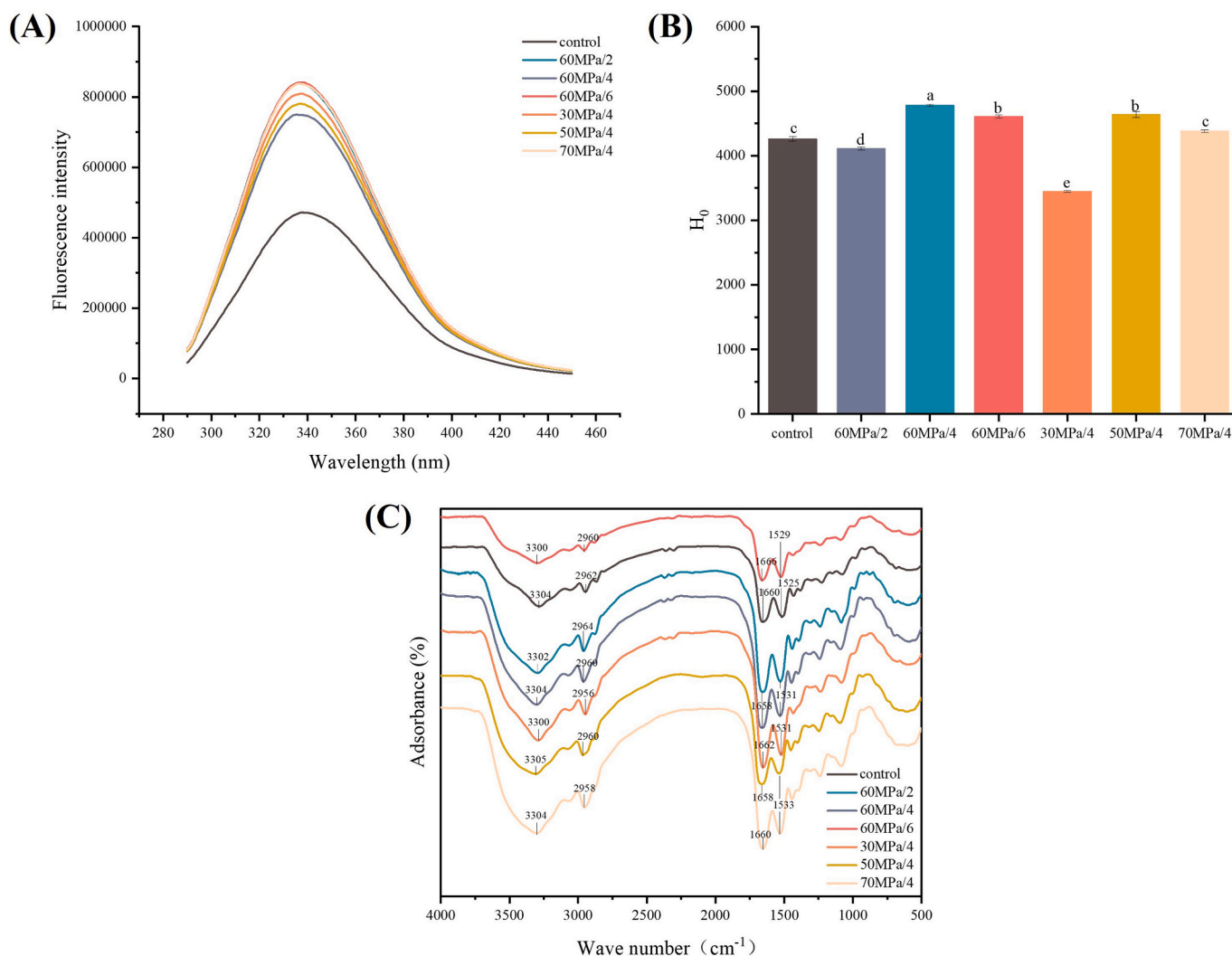


Fig. 2. Structural characterization of casein-polysaccharide complexes under different HPH intensities. (A): Fluorescence emission spectra. (B): Surface hydrophobicity. Note: Different letters on the bars indicate significant differences ($P < 0.05$). (C): FTIR spectrum.

Including the reactive amine groups previously buried in the inner parts of compact structure of proteins.

3.1.4. Fourier transform infrared spectroscopy (FTIR) analysis

The structural changes in casein were analyzed using FTIR spectroscopy (Fig. 2C). The four observed strong bands were attributed to amide A ($3,304 \text{ cm}^{-1}$), amide B ($2,960 \text{ cm}^{-1}$), amide I ($1,658 \text{ cm}^{-1}$), and amide II ($1,531 \text{ cm}^{-1}$). They correspond to the characteristic absorption peaks of O—H bonds, C—H bonds, C=O stretching, and N—H bending, respectively (Yu, Li, Sun, Yan, & Zou, 2022). All samples displayed similar characteristic absorption peaks. This indicated that HPH treatment modified the chain structure and the distribution of functional groups in the protein without changing the functional group types. This may suggest that casein binds more avidly to polysaccharides through hydrogen bonds. In comparison to the control, when the homogenization pressure was fixed, the peak heights of amides A, B, I, and II initially declined and then rose as the number of passes increased. Meanwhile, when the number of passes was fixed, the peak heights of amides A, B, I, and II initially declined as the homogenization pressure increased. Although there is a slight fluctuation at 50 MPa/4 times. This was attributed to an increased loss of molecular order (Wan et al., 2023). Changes in hydrogen bonding were possibly responsible for this phenomenon. Hydrogen bonds may arise from the connections between hydroxyl groups in polysaccharides and polar residues in casein, such as

glutamic acid, aspartic acid, serine, and threonine. Additionally, they can form by attaching to amine and carbonyl groups in the backbone. The spectra of the amide I band were analyzed to quantify the secondary structure of casein (α -helix, β -sheet, β -turn, and random coil) (Cheng et al., 2024). The variations in the secondary structure indicated substantial changes in the hydrogen bonds between the carbonyl and amide groups on the protein skeleton (Cheng et al., 2024). As shown in Table 1, HPH treatment depicted the expected structural reorganization. Compared with the control, the α -helix and β -sheet of the sample could be interconverted when the HPH intensity did not exceed 60 MPa/4 times. This indicated that HPH promoted the unfolding and rearrangements of the casein secondary structure, which led to changes in the orientation of protein hydrogen bonds. The main reason is that HPH could cause changes in the dihedral angle of the polypeptide chain, which led to a continuous change in the bond length of the hydrogen bond between C=O and N—H groups. The secondary structure of the sample revealed a transformation from β -turn to β -sheet when HPH intensity exceeded 60 MPa/4 times. This implied the transformation of the weak hydrogen bond structure to a strong hydrogen bond structure (Aziznia, Askari, Emamdjomeh, & Salami, 2024). Moreover, this represents a conformational transformation from ordered rigid structures to disordered flexible frameworks according to Wan et al. (2023).

Table 1
Secondary structure contents of casein–polysaccharide complexes under different HPH intensities.

	α -helix (%)	β -sheet (%)	β -turn (%)	Random coil (%)
control	18.32 \pm 0.05 ^c	33.53 \pm 0.07 ^b	30.83 \pm 0.07 ^a	17.31 \pm 0.07 ^b
60 MPa/2	18.67 \pm 0.07 ^b	33.02 \pm 0.09 ^{cd}	30.57 \pm 0.14 ^a	17.72 \pm 0.07 ^{ab}
60 MPa/4	18.77 \pm 0.13 ^{ab}	32.58 \pm 0.36 ^d	30.85 \pm 0.21 ^a	17.78 \pm 0.52 ^a
60 MPa/6	18.96 \pm 0.20 ^a	34.57 \pm 0.29 ^a	28.78 \pm 0.35 ^c	17.67 \pm 0.37 ^{ab}
30 MPa/4	18.34 \pm 0.11 ^c	33.31 \pm 0.14 ^{bc}	30.56 \pm 0.21 ^a	17.70 \pm 0.19 ^{ab}
50 MPa/4	18.36 \pm 0.19 ^c	33.12 \pm 0.73 ^c	30.78 \pm 0.19 ^a	17.72 \pm 0.08 ^{ab}
70 MPa/4	18.74 \pm 0.16 ^{ab}	33.25 \pm 0.18 ^c	30.23 \pm 0.23 ^b	17.75 \pm 0.20 ^{ab}

Note: Comparisons were carried out between values of the same column. Values with different letter indicate a significant difference at $P < 0.05$.

3.1.5. Sulfhydryl content and disulfide-bond analysis

The change in the sulfhydryl contents and disulfide bonds of casein, an important indicator of protein stability, can affect the interfacial properties and emulsifying ability of casein–polysaccharide complexes. As shown in Table 2, the total-sulfhydryl of the samples treated with HPH was significantly reduced ($P < 0.05$). This may be due to the rapid oxidation of cysteine residues forming sulfhydryl compounds while undergoing HPH treatment (Wang et al., 2024). As the HPH intensity increasing, the disulfide-bonds content of the samples first decreased, increased and then decreased, and the free-sulfhydryl content of the samples first increased, decreased and then increased. Among them, the disulfide-bonds content of the sample reached the highest value and the free-sulfhydryl content reached the lowest value at HPH intensity of 60 MPa/4 times. This was mainly due to the cavitation effect generated during the application of HPH, causing the oxidation of free thiol groups to disulfide bonds. Moreover, previous studies suggested that the second-largest forces to maintain the composite structure of casein and carrageenan were covalent disulfide bonds (Tang, Zhu, Li, Adhikari, & Wang, 2019). With an increase in HPH intensity, carrageenan was coiled into a spiral shape, and its sulfur-containing region was increased. This resulted in the enhancement of the disulfide bond between casein and carrageenan. Together, HPH treatment could promote the formation of disulfide bonds under appropriate intensity. Compared with the samples treated at 60 MPa/4 times, the samples treated at a higher HPH intensity (60 MPa/6 times and 70 MPa/4 times) showed a decrease in the total-sulfhydryl and disulfide-bond content with an increase in the free-

Table 2
Disulfide-bond and sulfhydryl contents of casein–polysaccharide complexes under different HPH intensities.

	Disulfide-bond ($\mu\text{mol/g}$)	Free-sulfhydryl ($\mu\text{mol/g}$)	Total-sulfhydryl ($\mu\text{mol/g}$)
control	12.54 \pm 0.36 ^b	21.64 \pm 0.53 ^e	34.18 \pm 0.19 ^a
60 MPa/2	4.12 \pm 0.51 ^f	26.65 \pm 0.61 ^a	30.75 \pm 0.47 ^{de}
60 MPa/4	13.50 \pm 0.23 ^a	20.07 \pm 0.24 ^e	33.57 \pm 0.29 ^b
60 MPa/6	9.04 \pm 0.56 ^{cd}	22.46 \pm 0.41 ^d	31.50 \pm 0.36 ^{cd}
30 MPa/4	6.87 \pm 0.47 ^e	23.60 \pm 0.47 ^b	30.47 \pm 0.27 ^e
50 MPa/4	8.30 \pm 0.52 ^d	23.34 \pm 0.74 ^b	31.63 \pm 0.49 ^c
70 MPa/4	9.86 \pm 0.72 ^c	21.04 \pm 0.76 ^f	30.90 \pm 0.68 ^{cde}

Note: Comparisons were carried out between values of the same column. Values with different letter indicate a significant difference at $P < 0.05$.

sulfhydryl content. This may be attributed to the further increase in the HPH intensity disrupting intermolecular disulfide bonds, thus exposing internal SH groups to the casein surface (Karabulut et al., 2024).

3.2. Interfacial properties of casein–polysaccharide complexes

3.2.1. Contact angle (θ) analysis

The wettability of particles is considered the main parameter controlling the interfacial behaviors and emulsifying properties of protein–polysaccharide complexes. An angle of 90° represents the optimal amphiphilicity of the composite particles, allowing for simultaneous infiltration by both oil and water. This leads to the spontaneous aggregation of particles at the interface, resulting in the formation of a rigid particle network structure. Moreover, this can effectively prevent droplet aggregation and play a role in interface stability in the D-FSMP system. The θ of samples tended to increase first and then decrease, with the increasing HPH intensity, as shown in Fig. 3A. The θ of the sample treated at 60 MPa/4 times was 90.89°, which was close to 90°. In this situation, the wettability of casein–polysaccharide complexes particles reached nearly the hydrophilic–lipophilic balance, leading to enhanced particle-adsorption at the interface. This contributed to creating a physical obstacle that impeded the aggregation of oil droplets (Zhang et al., 2023). The θ of other samples was significantly reduced ($P < 0.05$) compared with that of the control. This indicated that they exposed more hydrophilic groups than hydrophobic groups, which may be detrimental to the stability of the D-FSMP system (Tavasoli, Maghsoudlou, Shahiri Tabarestani, & Mahdi Jafari, 2023).

3.2.2. Interfacial tension analysis

Interfacial tension could be used to estimate the bonding strength and the stability of casein–polysaccharide complexes particles at the interface in the D-FSMP system. The adsorption behavior of particles at the oil–water interface required three processes: diffusion, expansion, and rearrangement. In general, the shorter the adsorption time and lower the interfacial tension, the greater the adsorption capacity of the particles (Soltani & Madadlou, 2015). As shown in Fig. 3B, the interfacial tension of all samples first exhibited a rapid decrease with time. Thereafter, the interfacial tension decreased slowly and gradually reached equilibrium. The process of interfacial tension decreasing to the equilibrium point with time was the adsorption process of particles at the oil–water interface. The interfacial tension initially exhibited a decreasing trend and then increased with the increasing HPH intensity; moreover, the time for the interfacial tension to reach equilibrium was gradually advanced. The interfacial tension of the sample treated at 60 MPa/4 times decreased the most, and it more quickly reached equilibrium. Proteins that were more amphiphilic exhibited a lower energy adsorption barrier and were able to diffuse faster at the oil–water interface, resulting in lower interfacial tension values (Wierenga, Meinders, Egmond, Voragen, & De Jongh, 2003). Moreover, a smaller protein particle-size was reported to promote interfacial adsorption. This is beneficial for the adsorption and ordered arrangement of casein–polysaccharide complexes at the oil–water interface, leading to a decrease in the interface free energy and the enhancement of interface stability. The excessively high HPH intensity resulted in the change in casein conformation from a flexible structure to a rigid structure and an increase in the hydrophilicity and size of casein–polysaccharide complexes. This restricted the adsorption of the adsorbed casein–polysaccharide complexes at the interface, resulting in an increased surface tension. This could be detrimental to the stability of the D-FSMP system.

3.2.3. EAI and ESI analysis

Both EAI and ESI were crucial indicators for assessing the emulsification capabilities of casein–polysaccharide complexes. A higher EAI value indicated that a unit mass of casein could stabilize a larger

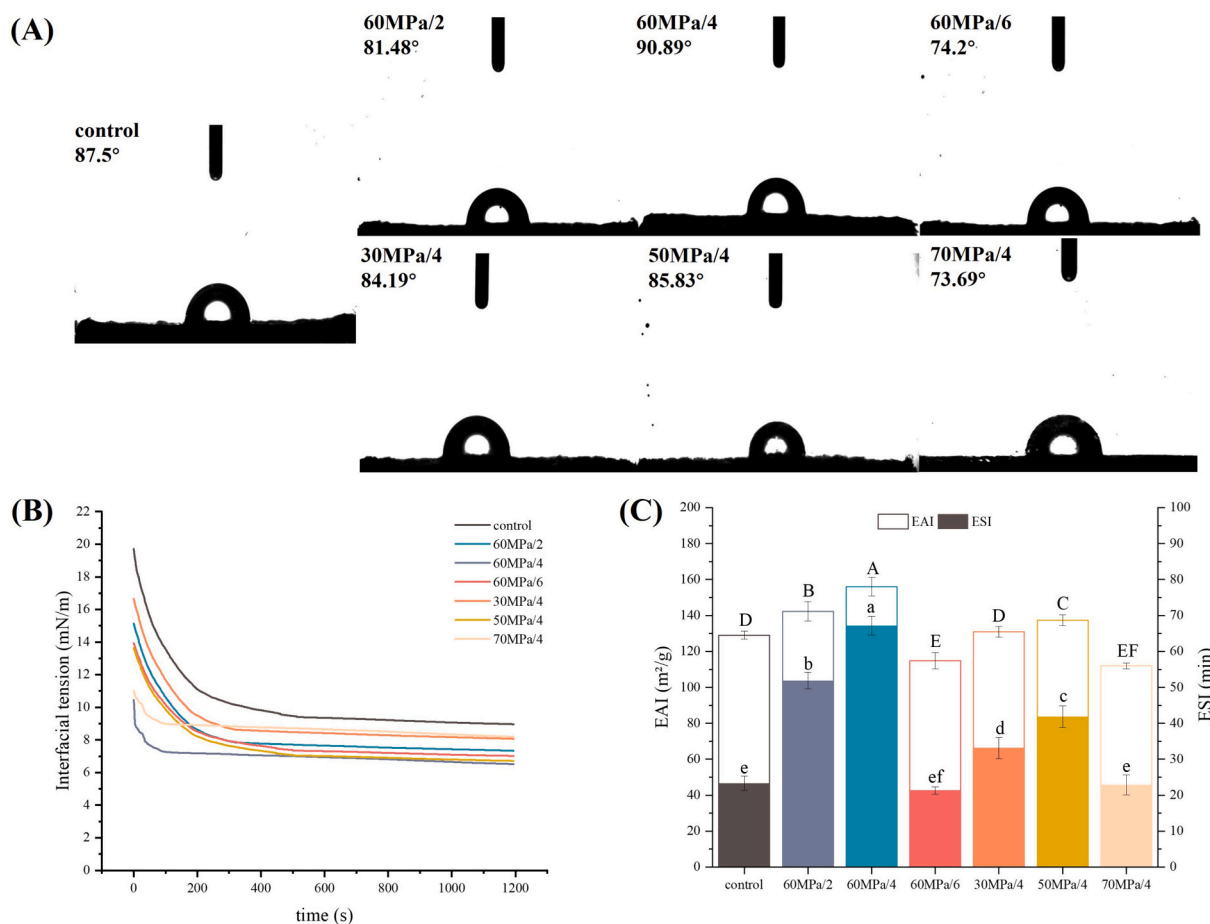


Fig. 3. Interfacial properties of casein-polysaccharide complexes under different HPH intensities. (A): Three-phase contact angle (θ). (B): Interfacial tension. (C): EAI and ESI. Note: Different lowercase letters on the bars indicate significant differences ($P < 0.05$) of the ESI; different uppercase letters on the bars indicate significant differences ($P < 0.05$) of the EAI.

oil-water interface area. The greater the ESI values, the longer the time for casein to stabilize the oil-water interface. Throughout emulsification, the emulsifying properties of proteins might be affected by the changes in their spatial structure. In Fig. 3C, compared with the control, the EAI and ESI of samples initially increased and then decreased with an increase in HPH intensity. The EAI and ESI of the sample reached the highest value when the sample was treated at 60 MPa/4 times. This improvement may be credited to the revolutionary influence of HPH on emulsions. According to reports, the EAI of proteins is strongly linked to their flexibility, and the strength of protein films significantly impacts the stability of food emulsions (Aryee, Agyei, & Udenigwe, 2018). Commonly, proteins or protein-polysaccharide complexes that are highly flexible often exhibit an improved EAI. Amino acid residues are able to swiftly reorganize and get absorbed at the oil-water interface owing to their ease of unfolding. Low structural flexibility would restrain proteins from unfolding and forming films around dispersed oil droplets. The current research found that the appropriate HPH intensity enhanced structural flexibility of casein and amphiphilicity. In addition, a higher H_0 was noted to be beneficial for particles to rearrange at the oil-water interface, forming a high-strength interface layer (Lisuzzo, Cavallaro, Milioto, & Lazzara, 2022). Therefore, the EAI and ESI increased. Excessive HPH intensity promoted the aggregation of casein-polysaccharide complexes, potentially reducing their flexibility and increasing their interfacial tension. Thus, by reducing the adsorption at the water/oil interface, the EAI and ESI be decreased.

3.3. The D-FSMP system stability analysis

3.3.1. Particle-size distribution analysis

The effect of different HPH intensities on the stability of the D-FSMP system was evaluated via particle size distribution. Commonly, a wider particle-size distribution could readily cause mutual aggregation between droplets. As shown in Fig. 4A, as the HPH intensity increased, the sample particle-size distribution shifted toward smaller particles. The peak type was gradually sharp and concentrated when the sample was treated at 60 MPa/4 times, indicating a more uniform droplet size distribution. This was presumably related to the smaller particle-size of the casein-polysaccharide complexes obtained under this treatment condition. Because the higher diffusion coefficient, rate of interface coverage, and interfacial strength of smaller particles compared to larger particles (Zhao, Fan, Li, & Zhong, 2024). An increased adsorption of casein and oil at the interface prevents the accumulation of droplets, resulting in improved emulsification capabilities. Nevertheless, the excessive shear force and cavitation effect disrupted the amphiphilicity of the casein-polysaccharide complexes, such as the samples treated at 60 Mpa/6 and 70 Mpa/4. This hindered the adsorption and structural relaxation rearrangement of complex particles at the oil-water interface. Therefore, the particle-size distribution broadened, which might decrease the stability of D-FSMP.

3.3.2. Zeta-potential analysis

The stability of emulsions has been demonstrated to be significantly influenced by the zeta-potential, which reflects the level of attraction or repulsion of the particles in suspension (Hilmi, Abushama, Abdalgadir,

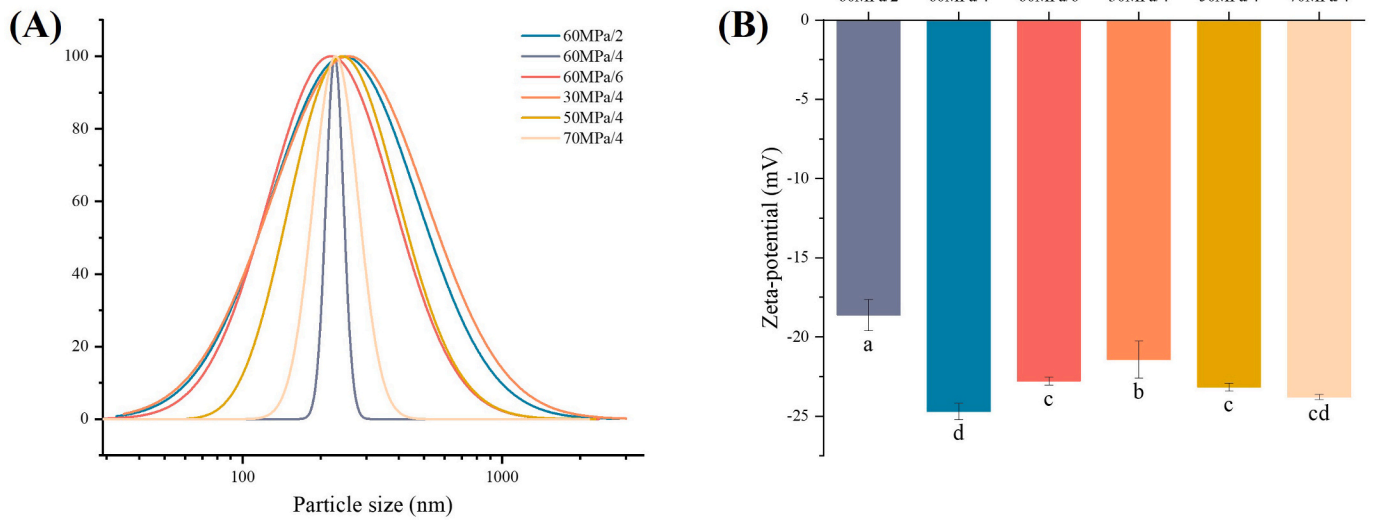


Fig. 4. (A): Particle-size distribution of D-FSMP products under different HPH intensities. (B): Zeta-potential of D-FSMP products under different HPH intensities. Note: Different letters on the bars indicate significant differences ($P < 0.05$).

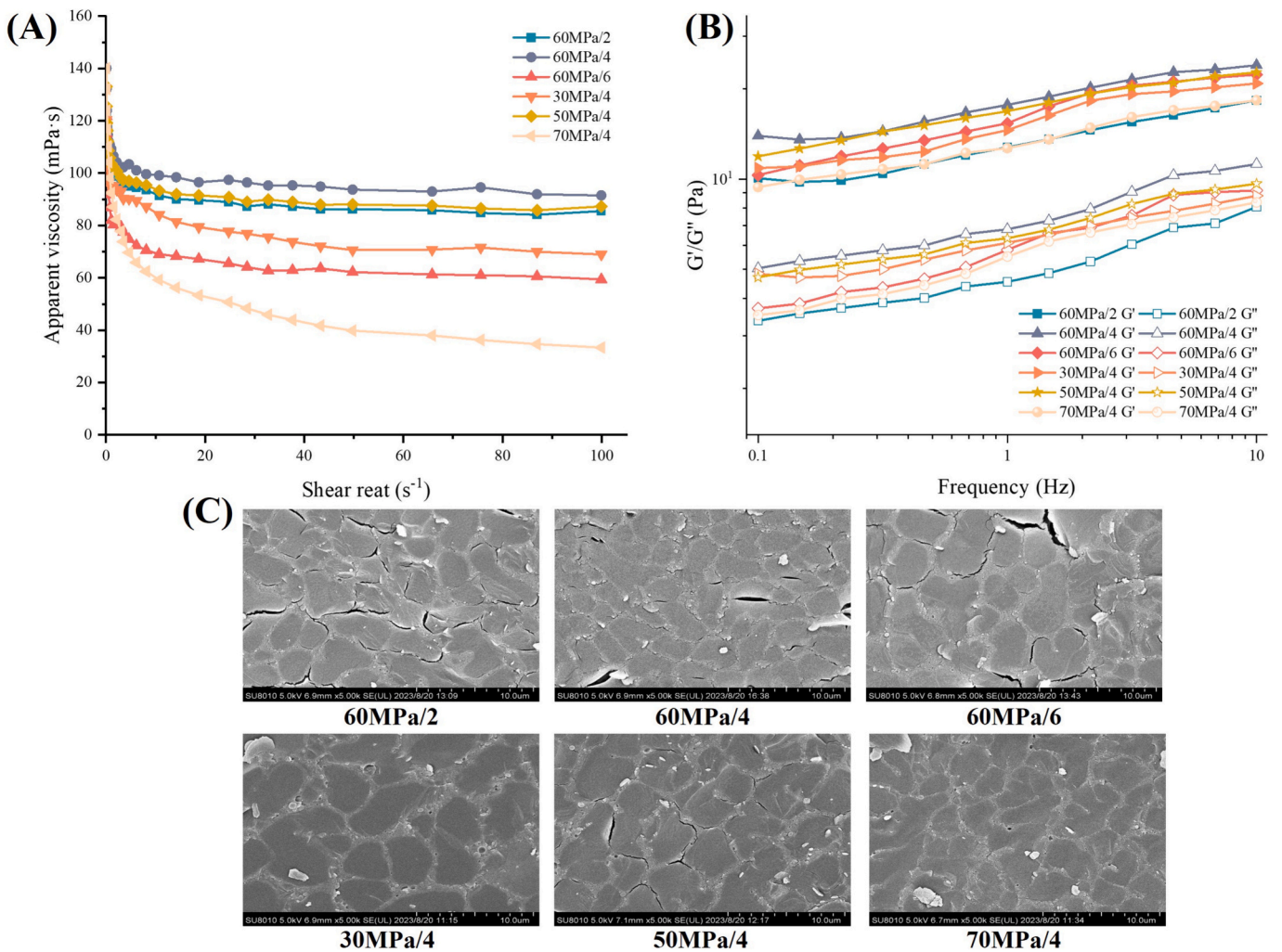


Fig. 5. (A): Apparent viscosity of D-FSMP products under different HPH intensities. (B): Rheological properties of D-FSMP products under different HPH intensities. (C): Cryo-SEM images of D-FSMP products under different HPH intensities.

Khalid, & Khalid, 2014). Typically, higher absolute values of zeta-potential indicate stronger intermolecular electrostatic repulsion, which serves to maintain emulsion stability and reduce droplet aggregation. Conversely, emulsion was prone to flocculation or creaming during storage. As seen in Fig. 4B, the zeta-potential of all samples was negative, and with a gradual increase in HPH intensity, the absolute value of the zeta-potential of the D-FSMP sample initially increased and then decreased. The absolute value of the zeta-potential of the sample treated at 60 MPa/4 times was the largest, which was 24.69 mV. This suggested that appropriate HPH intensity can enhance the surface charges of oil droplets by facilitating the exposure of additional ionizable protein groups and promoting protein adsorption at the interface. The casein-polysaccharide complexes could provide a higher intermolecular electrostatic-repulsion and energy barrier between the droplets. This could be one of the main reasons for the narrowing of the particle-size distribution of the sample treated at 60 MPa/4 times. However, excessive application of HPH intensity may produce opposite effects.

3.3.3. Apparent viscosity analysis

The apparent viscosity of the D-FSMP system has been abundantly associated with its stability. Higher apparent viscosity could effectively prevent droplet aggregation, which was conducive to the stability of the emulsion system. As shown in Fig. 5A, all samples displayed the characteristic non-Newtonian pseudoplastic-fluid and shear-thinning behavior. There is a possibility that the shear-thinning behavior was the result of the distortion/disorientation of ordered droplet structures, including the interface layer, during shearing, as explained by Saiki, Prestidge, and Horn (2007). The apparent viscosity of the sample first increased and then decreased with increasing HPH intensity. The apparent viscosity of the sample reached the highest value when the sample was treated at 60 MPa/4 times. Additional studies have revealed that appropriate HPH treatment was suitable for unfolding proteins and forming a network through intermolecular disulfide bonds and hydrophobic interactions, which thickened the continuous phase (Falade, Mu, & Zhang, 2021). This could be one reason for the increase in the apparent viscosity of the sample. Alternatively, it could be attributed to the reduction in the sample particle-size and the narrowing of size distribution because more the number of droplets under the same volume fraction, smaller the average distance between the droplets in the dispersed phase. Stokes' law states that the larger the volume of a protein solution, the greater the internal resistance to the flow of the solution (Wu et al., 2023). The excessively high HPH intensity resulted an increase in the sample particle-size and droplet spacing. This may reduce the effective volume fraction and flow resistance in the emulsion system, resulting in the reduction in the apparent viscosity of the samples (Hu, Tan, Julian McClements, & Wang, 2022).

3.3.4. Rheological property analysis

The rheological properties are related to the adsorption capacity, flexibility, and aggregation behavior of casein-polysaccharide complexes. They exert an important influence on the stability of the D-FSMP system. As shown in Fig. 5B, in the linear viscoelastic region, the elastic modulus (G') of all emulsions was greater than the corresponding loss modulus (G''). All samples exhibited elastic behavior. The G' and G'' values of the sample initially increased and then decreased with increasing HPH intensity. The G' and G'' values reached their highest values when the sample was treated at 60 MPa/4 times; this implies that HPH treatment played a positive role in contributing to the improvement of the network structure and viscoelasticity of the emulsions. This may be due to the fact that the conformation of casein was more relaxed and flexibility increased, further enhancing the structural stretchability of casein (Ruíz-Henestrosa et al., 2007). On the one hand, it promoted the interaction between casein and polysaccharide molecules at the interface, thereby enhancing the mechanical strength and resistance to deformation of the interfacial layer. On the other hand, it reduced the steric hindrance effect of casein-polysaccharide macromolecules. The

adsorption of casein-polysaccharide complexes at the oil-water interface was increased. Thus, the values of G' and G'' increased. The results of the analysis of the interfacial tension and θ were supportive of this inference.

3.3.5. Cryo-SEM

The cryo-SEM images distinctly revealed the formation of an obvious network structure around the droplets, as presented in Fig. 5C. Casein or the casein-polysaccharide complexes accumulated at the droplet interface. With a gradual increase in HPH intensity, the droplets of the emulsion first showed an increasing trend and then a decreasing trend. The cavitation effect caused by appropriate HPH intensity (60 MPa/4 times) led to a change in casein conformation, which may expose the active groups ($-\text{OH}$, $-\text{COOH}$, $-\text{NH}_2$) and hydrophobic fragments on the side chains of casein molecules (Yang et al., 2024). Moreover, it promoted physical interaction between casein-casein and casein-polysaccharide complexes to construct an adhesion interface and connect with each other to form a network. The three-dimensional network structure prevented the flocculation and coalescence of adjacent emulsion droplets by acting as steric barriers. However, obvious evidence of droplet coalescence was observed in samples treated at 60 MPa/6 times and 70 MPa/4 times. Thus, their droplet size distribution was observed to be uneven. This indicated that the poor resistance to deformation of the interface network structure is caused by excessively high HPH intensity, which is not conducive to stabilizing the D-FSMP system (Hu et al., 2023).

3.4. Appearance changes of D-FSMP products after storage

The storage stability of D-FSMP products was observed by storing all samples at room temperature for 1 month to determine the effect of different HPH intensities. As shown in Fig. 6, the control without HPH treatment formed a severely layered emulsion (this is the reason why the group of samples was not assessed in Section 3.3), whereas samples treated with HPH formed a normal emulsion. The whitish layer on the surface of the samples initially decreased and then increased with increasing HPH intensity. The lower the height of the white layer, the higher the storage stability of D-FSMP products. When the sample was treated at 60 MPa/4 times, HPH could effectively improve its storage stability by constructing a stable D-FSMP system. This was mainly due to its influence on the structure, interface properties, and emulsifying properties of the casein-polysaccharide complexes.

4. Conclusion

As per our findings, the stability of D-FSMP could be effectively improved by HPH, and the process effect was the best at 60 MPa/4 times. This is mainly due to the fact that it can effectively improve the structural flexibility of casein molecules and promote the formation of smallest sized casein-polysaccharide complexes (mainly through hydrogen bonding and hydrophobic interactions). The casein-polysaccharide complexes exhibited nearly neutral wettability, lower interfacial tension, and the highest emulsifying activity. Therefore, its apparent viscosity and viscoelasticity were effectively improved, and the resistance to the deformation of the interface network was also enhanced. However, excessive homogenization pressure and number of passes were not conducive to the stability of the D-FSMP system. The results presented here would be beneficial for the application of HPH to structurally modify protein-polysaccharide complexes for desirable stability of the D-FSMP system. However, the interfacial adsorption mechanism and behavior of casein-polysaccharide complexes were not characterized in this work. This still needs to be further explored.

CRedit authorship contribution statement

Xueting Zheng: Writing – original draft, Software,



Fig. 6. Appearance changes of D-FSMP products after 1 month of storage under different HPH intensities.

Conceptualization. **Zengwang Guo**: Project administration, Funding acquisition. **Jiayu Zhang**: Data curation. **Tianfu Cheng**: Resources, Funding acquisition. **Hong Yang**: Writing – review & editing. **Wentao Zhang**: Methodology, Investigation. **Linyi Zhou**: Visualization, Validation, Supervision.

Declaration of competing interest

The authors declare that they have no known competing financial interests or personal relationships that could have appeared to influence the work reported in this paper.

Data availability

Data will be made available on request.

Acknowledgments

This work was supported by the National Key Research and Development Program of China [2022YFF1100600]; the National Key Research and Development Program of China [2022YFF1101500]; the Heilongjiang Province announces and leads scientific and technological research projects [2023XJ08B02].

Appendix A. Supplementary data

Supplementary data to this article can be found online at <https://doi.org/10.1016/j.fochx.2024.101695>.

References

- Aljewicz, M., Keklik, M., Recio, I., & Martínez-Sanz, M. (2024). Effect of polysaccharide-protein interactions on the multi-scale structure of hybrid micellar casein-xanthan gum systems. *Food Hydrocolloids*, *151*, Article 109833. <https://doi.org/10.1016/j.foodhyd.2024.109833>
- Aryee, A. N. A., Agyei, D., & Udenigwe, C. C. (2018). 2—Impact of processing on the chemistry and functionality of food proteins. In R. Y. Yada (Ed.), *Proteins in food processing* (2nd ed., pp. 27–45). Woodhead Publishing. <https://doi.org/10.1016/B978-0-08-100722-8.00003-6>.
- Aziznia, S., Askari, G., Emamdjomeh, Z., & Salami, M. (2024). Effect of ultrasonic assisted grafting on the structural and functional properties of mung bean protein isolate conjugated with maltodextrin through maillard reaction. *International Journal of Biological Macromolecules*, *254*, Article 127616. <https://doi.org/10.1016/j.ijbiomac.2023.127616>
- Bakwo Bassogog, C. B., Nyobe, C. E., Ngui, S. P., Minka, S. R., & Mune Mune, M. A. (2022). Effect of heat treatment on the structure, functional properties and composition of *Moringa oleifera* seed proteins. *Food Chemistry*, *384*, Article 132546. <https://doi.org/10.1016/j.foodchem.2022.132546>
- Burgos-Díaz, C., Wandersleben, T., Marqués, A. M., & Rubilar, M. (2016). Multilayer emulsions stabilized by vegetable proteins and polysaccharides. *Current Opinion in Colloid & Interface Science*, *25*, 51–57. <https://doi.org/10.1016/j.cocis.2016.06.014>
- Cámara-Martos, F., & Iturbide-Casas, M. (2019). 13 - Enteral nutrition formulas: Current evidence and nutritional composition. In A. M. Grumezescu, & A. M. Holban (Eds.), *Nutrients in beverages* (pp. 467–508). Academic Press. <https://doi.org/10.1016/B978-0-12-816842-4.00013-7>.

- Casale, R., Symeonidou, Z., Ferfeli, S., Micheli, F., Scarsella, P., & Paladini, A. (2021). Food for special medical purposes and nutraceuticals for pain: A narrative review. *Pain and therapy*, *10*(1), 225–242. <https://doi.org/10.1007/s40122-021-00239-y>
- Cheng, T., Tian, Y., Liu, C., Yang, H., Wang, Z., Xu, M., Guo, Z., & Zhou, L. (2024). Effect of xanthan gum (XG) and carrageenan (CG) ratio on casein (CA)-XG-CG ternary complex: Used to improve the stability of liquid diabetes formula food for special medical purposes. *International Journal of Biological Macromolecules*, Article 131770. <https://doi.org/10.1016/j.ijbiomac.2024.131770>
- Cheng, T., Wang, Z., Sun, F., Liu, H., Liu, J., Guo, Z., & Zhou, L. (2024). Gel properties of rice proteins-pectin composite and the delivery potential for curcumin: Based on different concentrations and the degree of esterification of pectin. *Food Hydrocolloids*, *146*, Article 109305. <https://doi.org/10.1016/j.foodhyd.2023.109305>
- Cheng, T., Zhang, G., Sun, F., Guo, Y., Ramakrishna, R., Zhou, L., Guo, Z., & Wang, Z. (2024). Study on stabilized mechanism of high internal phase Pickering emulsions based on commercial yeast proteins: Modulating the characteristics of Pickering particle via sonication. *Ultrasonics Sonochemistry*, *104*, Article 106843. <https://doi.org/10.1016/j.ulsonch.2024.106843>
- Chinese Diabetes Society & National Office for Primary Diabetes Care. (2022). National guidelines for the prevention and control of diabetes in primary care (2022). *Zhonghua Nei Ke Za Zhi*, *61*(3), Article 3. <https://doi.org/10.3760/cma.j.cn112138-20220120-000063>
- Dai, C., Han, S., Ma, C., McClements, D. J., Xu, D., Chen, S., ... Liu, F. (2024). High internal phase emulsions stabilized by pea protein isolate-EGCG-Fe³⁺ complexes: Encapsulation of β -carotene. *Food Hydrocolloids*, *150*, Article 109607. <https://doi.org/10.1016/j.foodhyd.2023.109607>
- Falade, E. O., Mu, T.-H., & Zhang, M. (2021). Improvement of ultrasound microwave-assisted enzymatic production and high hydrostatic pressure on emulsifying, rheological and interfacial characteristics of sweet potato protein hydrolysates. *Food Hydrocolloids*, *117*, Article 106684. <https://doi.org/10.1016/j.foodhyd.2021.106684>
- Hilmi, Y., Abushama, M. F., Abdalgadir, H., Khalid, A., & Khalid, H. (2014). A study of antioxidant activity, enzymatic inhibition and in vitro toxicity of selected traditional sudanese plants with anti-diabetic potential. *BMC Complementary and Alternative Medicine*, *14*(1), Article 1. <https://doi.org/10.1186/1472-6882-14-149>
- Hu, J., Yu, B., Yuan, C., Tao, H., Wu, Z., Dong, D., Lu, Y., Zhang, Z., Cao, Y., Zhao, H., Cheng, Y., & Cui, B. (2023). Influence of heat treatment before and/or after high-pressure homogenization on the structure and emulsification properties of soybean protein isolate. *International Journal of Biological Macromolecules*, *253*, Article 127411. <https://doi.org/10.1016/j.ijbiomac.2023.127411>
- Hu, Y., Tan, Y., Julian McClements, D., & Wang, L. (2022). Fabrication, characterization and *in vitro* digestive behavior of Pickering emulsion incorporated with dextrin. *Food Chemistry*, *384*, Article 132528. <https://doi.org/10.1016/j.foodchem.2022.132528>
- Huang, L., Lu, J., Shi, L., & Zhang, H. (2023). Regulation, production and clinical application of foods for special medical purposes (FSMPs) in China and relevant application of food hydrocolloids in dysphagia therapy. *Food Hydrocolloids*, *140*, Article 108613. <https://doi.org/10.1016/j.foodhyd.2023.108613>
- Jiang, H., Zhang, T., Pan, Y., Yang, H., Xu, X., Han, J., & Liu, W. (2024). Thermal stability and *in vitro* biological fate of lactoferrin-polysaccharide complexes. *Food Research International*, *182*, Article 114182. <https://doi.org/10.1016/j.foodres.2024.114182>
- Karabulut, G., Kapoor, R., Yemis, O., & Feng, H. (2024). Manothermosonication, high-pressure homogenization, and their combinations with pH-shifting improve the techno-functionality and digestibility of hemp protein. *Food Hydrocolloids*, *150*, Article 109661. <https://doi.org/10.1016/j.foodhyd.2023.109661>
- Lisuzzo, L., Cavallaro, G., Milioto, S., & Lazzara, G. (2022). Pickering emulsions stabilized by halloysite nanotubes: From general aspects to technological applications. *Advanced Materials Interfaces*, *9*(10), Article 10. <https://doi.org/10.1002/admi.202102346>
- Lu, Y., Zhang, Y., Yuan, F., Gao, Y., & Mao, L. (2021). Emulsion gels with different proteins at the interface: Structures and delivery functionality. *Food Hydrocolloids*, *116*, Article 106637. <https://doi.org/10.1016/j.foodhyd.2021.106637>
- Machado, J. P. E., Benyahia, L., & Nicolai, T. (2021). Effect of adding a third polysaccharide on the adsorption of protein microgels at the interface of polysaccharide-based water in water emulsions. *Journal of Colloid and Interface Science*, *603*, 633–640. <https://doi.org/10.1016/j.jcis.2021.06.053>

- Nagasawa, Y., Katagiri, S., Nakagawa, K., Hirota, T., Yoshimi, K., Uchida, A., Hatasa, M., Komatsu, K., Shiba, T., Ohsugi, Y., Uesaka, N., Iwata, T., & Tohara, H. (2022). Xanthan gum-based fluid thickener decreases postprandial blood glucose associated with increase of *Glp1* and *Glp1r* expression in ileum and alteration of gut microbiome. *Journal of Functional Foods*, 99, Article 105321. <https://doi.org/10.1016/j.jff.2022.105321>
- Plazzotta, S., Moreton, M., Calligaris, S., & Manzocco, L. (2021). Physical, chemical, and techno-functional properties of soy okara powders obtained by high pressure homogenization and alkaline-acid recovery. *Food and Bioprocess Technology*, 128, 95–101. <https://doi.org/10.1016/j.fbp.2021.04.017>
- Pohl, M., Mayr, P., Merti-Roetzer, M., Lauster, F., Lerch, M., Eriksen, J., ... Rahlfs, V. W. (2005). Glycaemic control in type II diabetic tube-fed patients with a new enteral formula low in carbohydrates and high in monounsaturated fatty acids: A randomised controlled trial. *European Journal of Clinical Nutrition*, 59(11), Article 11. <https://doi.org/10.1038/sj.ejcn.1602232>
- Ruíz-Henestrosa, V. P., Sánchez, C. C., Escobar, M., del, M. Y., Jiménez, J. J. P., Rodríguez, F. M., & Patino, J. M. R. (2007). Interfacial and foaming characteristics of soy globulins as a function of pH and ionic strength. *Colloids and Surfaces A: Physicochemical and Engineering Aspects*, 309(1), Article 1. <https://doi.org/10.1016/j.colsurfa.2007.01.030>
- Ruperto, M., Montero-Bravo, A., Partearroyo, T., Puga, A. M., Varela-Moreiras, G., & Samaniego-Vaesken, M. de L. (2022). A descriptive analysis of macronutrient, fatty acid profile, and some immunomodulatory nutrients in standard and disease-specific enteral formulae in Europe. *Frontiers in Nutrition*, 9, Article 877875. <https://doi.org/10.3389/fnut.2022.877875>
- Saiki, Y., Prestidge, C. A., & Horn, R. G. (2007). Effects of droplet deformability on emulsion rheology. *Colloids and Surfaces A: Physicochemical and Engineering Aspects*, 299(1), Article 1. <https://doi.org/10.1016/j.colsurfa.2006.11.022>
- Soltani, S., & Madadlou, A. (2015). Gelation characteristics of the sugar beet pectin solution charged with fish oil-loaded zein nanoparticles. *Food Hydrocolloids*, 43, 664–669. <https://doi.org/10.1016/j.foodhyd.2014.07.030>
- Stippler, D., Bode, V., Fischer, M., Kollex, K., Rohde, E., Tisowsky, B., Küstner, J., & Pahne, N. (2015). Proposal for a new practicable categorization system for food for special medical purposes – Enteral nutritional products. *Clinical Nutrition ESPEN*, 10(6), e219–e223. <https://doi.org/10.1016/j.clnesp.2015.07.003>
- Tang, M., Zhu, Y., Li, D., Adhikari, B., & Wang, L. (2019). Rheological, thermal and microstructural properties of casein/ κ -carrageenan mixed systems. *LWT*, 113, Article 108296. <https://doi.org/10.1016/j.lwt.2019.108296>
- Tao, L., Wang, H., Wang, J., Zhang, J., Yu, L., & Song, S. (2024). Characterization and emulsion stability of soybean protein isolate/soybean peptide and ginseng polysaccharide conjugates. *LWT*, 196, Article 115860. <https://doi.org/10.1016/j.lwt.2024.115860>
- Tavasoli, S., Maghsoudlou, Y., Shahiri Tabarestani, H., & Mahdi Jafari, S. (2023). Changes in emulsifying properties of caseinate–soy soluble polysaccharides conjugates by ultrasonication. *Ultrasonics Sonochemistry*, 101, Article 106703. <https://doi.org/10.1016/j.ultsonch.2023.106703>
- Tian, Y., Yuan, C., Cui, B., Lu, L., Zhao, M., Liu, P., Wu, Z., & Li, J. (2022). Pickering emulsions stabilized by β -cyclodextrin and cinnamaldehyde essential oil/ β -cyclodextrin composite: A comparison study. *Food Chemistry*, 377, Article 131995. <https://doi.org/10.1016/j.foodchem.2021.131995>
- Wan, W., Feng, J., Wang, H., Du, X., Wang, B., Yu, G., & Xia, X. (2023). Influence of repeated freeze-thaw treatments on the oxidation and degradation of muscle proteins from mirror carp (*Cyprinus carpio* L.), based on myofibrillar protein structural changes. *International Journal of Biological Macromolecules*, 226, 454–462. <https://doi.org/10.1016/j.ijbiomac.2022.12.082>
- Wang, Q., Tang, Z., Cao, Y., Ming, Y., & Wu, M. (2024). Improving the solubility and interfacial absorption of hempseed protein via a novel high pressure homogenization-assisted pH-shift strategy. *Food Chemistry*, 442, Article 138447. <https://doi.org/10.1016/j.foodchem.2024.138447>
- Wang, S., Zheng, X., Zheng, L., Yang, Y., Xiao, D., Zhang, H., Ai, B., & Sheng, Z. (2023). κ -Carrageenan inhibits the formation of advanced glycation end products in cakes: Inhibition mechanism, cake characteristics, and sensory evaluation. *Food Chemistry*, 429, Article 136583. <https://doi.org/10.1016/j.foodchem.2023.136583>
- Wierenga, P. A., Meinders, M. B. J., Egmond, M. R., Voragen, F. A. G. J., & De Jongh, H. H. J. (2003). Protein exposed hydrophobicity reduces the kinetic barrier for adsorption of ovalbumin to the air–water interface. *Langmuir*, 19(21), Article 1. <https://doi.org/10.1021/la034868p>
- Wu, J., Tang, Y., Chen, W., Chen, H., Zhong, Q., Pei, J., Han, T., Chen, W., & Zhang, M. (2023). Mechanism for improving coconut milk emulsions viscosity by modifying coconut protein structure and coconut milk properties with monosodium glutamate. *International Journal of Biological Macromolecules*, 252, Article 126139. <https://doi.org/10.1016/j.ijbiomac.2023.126139>
- Wu, L., Zhang, L., & Zhang, Y. (2019). A review on rules for examination of licensing criteria for producing foods for special medical purpose in China. *Food Science and Human Wellness*, 8(2), 106–114. <https://doi.org/10.1016/j.fshw.2019.05.005>
- Yang, Y., Xu, Q., Wang, X., Bai, Z., Xu, X., & Ma, J. (2024). Casein-based hydrogels: Advances and prospects. *Food Chemistry*, 447, Article 138956. <https://doi.org/10.1016/j.foodchem.2024.138956>
- Yin, X., Gao, M., Wang, H., Chen, Q., & Kong, B. (2022). Probing the interaction between selected furan derivatives and porcine myofibrillar proteins by spectroscopic and molecular docking approaches. *Food Chemistry*, 397, Article 133776. <https://doi.org/10.1016/j.foodchem.2022.133776>
- Yu, C., Li, S., Sun, S., Yan, H., & Zou, H. (2022). Modification of emulsifying properties of mussel myofibrillar proteins by high-intensity ultrasonication treatment and the stability of O/W emulsion. *Colloids and Surfaces A: Physicochemical and Engineering Aspects*, 641, Article 128511. <https://doi.org/10.1016/j.colsurfa.2022.128511>
- Yu, Q., Wu, H., & Fan, L. (2024). Formation of casein and maltodextrin conjugates using shear and their effect on the stability of total nutrient emulsion based on homogenization. *Food Hydrocolloids*, 149, Article 109533. <https://doi.org/10.1016/j.foodhyd.2023.109533>
- Zhang, J.-B., Wu, N.-N., Yang, X.-Q., He, X.-T., & Wang, L.-J. (2012). Improvement of emulsifying properties of Maillard reaction products from β -conglycinin and dextran using controlled enzymatic hydrolysis. *Food Hydrocolloids*, 28(2), Article 2. <https://doi.org/10.1016/j.foodhyd.2012.01.006>
- Zhang, L., Zhou, C., Xing, S., Chen, Y., Su, W., Wang, H., & Tan, M. (2023). Sea bass protein-polyphenol complex stabilized high internal phase of algal oil Pickering emulsions to stabilize astaxanthin for 3D food printing. *Food Chemistry*, 417, Article 135824. <https://doi.org/10.1016/j.foodchem.2023.135824>
- Zhao, Q., Fan, L., Li, J., & Zhong, S. (2024). Pickering emulsions stabilized by biopolymer-based nanoparticles or hybrid particles for the development of food packaging films: A review. *Food Hydrocolloids*, 146, Article 109185. <https://doi.org/10.1016/j.foodhyd.2023.109185>